

## Mechanical Properties of Al<sub>2</sub>O<sub>3</sub> Particle-Reinforced A356 Composite Produced by a Multi-step Process Regime

Nattapat Kanchanaruangrong<sup>1</sup>, Sukangkana Talangkun<sup>2\*</sup>,  
Charuayporn Santhaweesuk<sup>1</sup> and Surachai Numsarapatnuk<sup>3</sup>

<sup>1</sup>Department of Industrial Engineering, Faculty of Engineering, Ubonratchathani University, Ubonratchathani 34190, Thailand

<sup>2</sup>Department of Industrial Engineering, Faculty of Engineering, Khon Kaen University, Khon Kaen 40002, Thailand

<sup>3</sup>Faculty of Engineering and Architecture, Rajamangala University of Technology Tawan-ok Uthenthawai Campus, Pathum Wan, Bangkok 10330, Thailand

\*Corresponding author. E-mail: sukangkana@kku.ac.th

### ABSTRACT

*The aim of this study was to produce a composite material of A356 aluminum alloy reinforced with 250 μm alumina (Al<sub>2</sub>O<sub>3</sub>) powder. A multi-step process regime was developed. Strain was induced via milling in production of A356 chips. The chips were dry mixed with Al<sub>2</sub>O<sub>3</sub> at 5, 10, and 15 wt% and cold pressed, followed by sintering at 600°C for 20 min. Then the molten composite was sand casted into a cylinder with a diameter of 20 mm and length of 50 mm. Afterward, all cast specimens were heat treated by solution treatment at 527°C for 12 h, quenched in water, and naturally aged at room temperature for 10 h; then artificially aged at 177°C for 12 h and furnace cooled. Specimens were subjected to hardness and wear tests. The results of hardness testing of the ‘as received’ A356 and casted A356-5, 10, and 15 wt% Al<sub>2</sub>O<sub>3</sub> were 23.5 HRB, 41.3 HRC, 44.0 HRC, and 46.0 HRC, respectively, and the average hardness values after heat treatment were 46.0 HRB, 46.3 HRC, 48.0 HRC, and 51.1 HRC, respectively. The percentage of Al<sub>2</sub>O<sub>3</sub> was a significant factor based on statistical analysis. The hardness values increased significantly after heat treatment. In addition, heat-treated A356-5, 10, and 15 wt% Al<sub>2</sub>O<sub>3</sub> exhibited average wear rates of 0.00387, 0.00375, and 0.00350 mm<sup>3</sup>/m, respectively. Increasing the amount of alumina reduced the wear rate, but the difference was not statistically significant. The cross-section micrographs revealed that the alumina powders were uniformly dispersed in A356 matrix.*

**Keywords:** A356/Al<sub>2</sub>O<sub>3</sub>, Strain-induced, Sintering, Hardness, Sand casting

### INTRODUCTION

Currently, aluminum metal matrix composites (AMMCs) have been widely studied and broadly accepted by industries as efficient alternative materials in many applications, especially as components in drum or disc brakes. Generally,

the matrix metal exhibits good ductility and impact strength, and high thermal and electrical conductivity. Most reinforcing materials are ceramics with high elastic modulus, and contribute to good fatigue and wear resistance. As with any composite material, AMMCs rely upon the combined characteristics of each component to achieve properties that are otherwise difficult to attain in any single class of material. The combination of properties can only be fully realized when the matrix and reinforcing material have the correct bonding properties. For instance, the interface characteristics between the materials are critical to determining whether loads are properly distributed on a microscopic level in a way that the forces are forward of the reinforcing material (Hashim et al., 2001).

A356 aluminum, an aluminum-silicon-magnesium alloy, has good casting properties and high toughness, corrosion resistance, machinability and strength-to-weight ratio. It is one of many aluminium alloys commonly used in industrial components that require high strength, such as aircraft parts, pump housings, impellers, and structural castings. In automotive applications, disk brakes are normally made from cast iron and stainless steel, which have high wear and corrosion resistance and good heat conductivity. However, disk brakes can also be produced using aluminum alloys reinforced with  $\text{Al}_2\text{O}_3$ , which can exhibit similar properties, but also are lightweight by comparison (Varuzan et al., 2002; Zhang and Wang, 2007). Al/SiC and Al/ $\text{Al}_2\text{O}_3$  composite products can be used to replace copper, steel, titanium, and cast iron components in several industries (Telang et al., 2010). AMMCs can reduce the weight of braking systems by 50-60 percent (Stephenson, 1996).

The properties of metal matrix composites that use particle reinforcement depend on several factors; for example, particle size, the amount and type of reinforcing phases, and the strength of the matrix-reinforced particle interface. Kok (2005) reinforced 2024 AMMCs with three different sizes and weight fractions of  $\text{Al}_2\text{O}_3$  particles up to 30 wt% fabricated by a vortex method with subsequent application of pressure. The coarser particles were more uniformly dispersed, while the finer particles formed agglomerations of particles and contributed to porosity. The hardness and the tensile strength of the composites increased with decreasing size and increasing weight fraction of particles.

Al/ $\text{Al}_2\text{O}_3$  composites have also been produced by conventional powder metallurgy, with pure aluminum powder with 10 wt% fine alumina sintered and compressed; the alumina showed better thermal stability at high temperatures (Rahimian et al., 2009). Composites containing  $\text{Al}_2\text{O}_3$  were superior to those containing SiC in abrasive wear resistance using a dry sand/rubber wheel abrasion tester, because of the formation of a brittle bonding layer at the interfaces between the aluminum matrix and SiC. Wear resistance of a composite containing large  $142\ \mu\text{m}$   $\text{Al}_2\text{O}_3$  was better than that of composites containing smaller  $\text{Al}_2\text{O}_3$  particles, and was comparable to AISI 1345 steel, heat treated to a hardness of 57 HRC (Bhansali and Mehrabian, 1982).

This study investigated the castability of A356/ $\text{Al}_2\text{O}_3$  composite produced via a multi-step regime – milling, sintering, rapid melting, and sand casting, as well analyzed the mechanical properties and microstructures of the various weight fractions.

## MATERIAL AND METHODS

### Materials

This experiment used commercial A356 aluminum alloy ingots. Chemical compositions were analyzed using Spark Emission Spectrometer (Model CI-4 P/N 081646, Baird, USA). The A356 consisted of Al, Si-7.23, Mg-0.31, Cu-0.036, Fe-0.107, Zn-0.005, Ti-0.153, and Ni-0.005 (wt%). The A356 aluminum alloy ingot was machined into small chips sizing approximately 4x7x0.1 mm before casting. The alumina (Al<sub>2</sub>O<sub>3</sub>) angular particles were commercial grade alumina (Great Rich Mineral Limited, China) with a uniform size of 250 μm. The theoretical mechanical properties of both materials are listed in Table 1.

**Table 1.** Typical physical and mechanical properties of A356 and Al<sub>2</sub>O<sub>3</sub> (Callister, 2007).

Materials	Density (g/cm <sup>3</sup> )	Tensile strength (MPa)	Modulus of elasticity (GPa)
A356	2.70	228.0	72.4
Aluminium Oxide (Al <sub>2</sub> O <sub>3</sub> )	3.98	416.0	380

### Composite compositions

The composites of A356 mixed with Al<sub>2</sub>O<sub>3</sub> were produced at weight fractions of 5, 10, and 15%. The density of each composite was computed by the following equation (Donald and Pradeep, 2009) and expressed as g/cm<sup>3</sup>:

$$\rho_c = \rho_m v_m + \rho_p v_p \tag{1}$$

where  $\rho_c$  is the composite's density,  $\rho_m$  is the matrix's density,  $v_m$  is the matrix's volume fraction,  $\rho_p$  is the reinforcing phase's density, and  $v_p$  is the reinforcing phase's volume fraction.

Volume fraction of composites was calculated by the followed equation and expressed as percentage.

$$v_c = \frac{1}{1 + \frac{\rho_p}{\rho_m} \left[ \frac{1}{w_p} - 1 \right]} \tag{2}$$

where,  $v_c$  is the composite's volume fraction and  $w_p$  is the reinforcing phase's weight fraction. Values of estimated density calculated from equation 1 and volume fraction calculated from equation 2 are listed in Table 2.

**Table 2.** Calculated volume fraction and density of composites.

Materials	Volume fraction (%)	Density (g/cm <sup>3</sup> )
A356-5wt% Al <sub>2</sub> O <sub>3</sub>	3.46	2.75
A356-10wt% Al <sub>2</sub> O <sub>3</sub>	6.92	2.79
A356-15wt% Al <sub>2</sub> O <sub>3</sub>	10.38	2.82

### The composite casting

A356 chips were dry mixed with alumina particles of 250  $\mu\text{m}$  and compressed into a small cylinder by hydraulic pressure as shown in Figure 1(A). To remove moisture and improve wettability between the alumina particles and aluminum, the compressed composite was sintered at 600°C for approximately 20 min in an electric furnace, and then transferred into an induction furnace and melted at 1,350°C. After 5 min holding time in the furnace without stirring, the molten composite was poured into a green sand mold and sand casted into a solid rod with a diameter of 20 mm and length of 50 mm as shown in Figure 1(B). Subsequently, all casted specimens were subjected to solution treatment at 527°C for 12 h, quenched into water, and then naturally aged at room temperature for 10 h; then artificially aged at 177°C for 12 h and slowly cooled in the furnace (Figure 2).

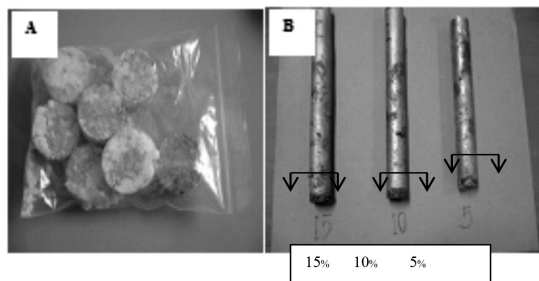


**Figure 1.** Photographs of the pressed composite mixture before sintering (A) and the casted sand composites with alumina of 5, 10, and 15 wt% (B).

Note: Arrows show positions for microscopy.

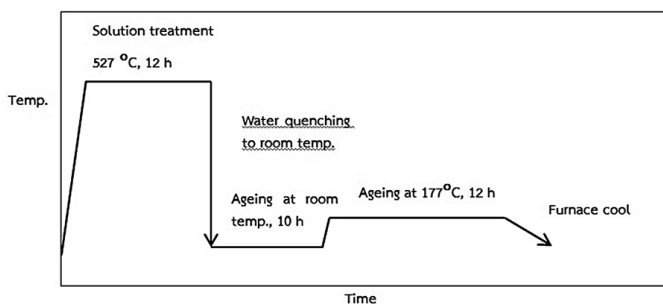


**Figure 2.** Heat treatment cycle.

### Microstructural characterization

Microstructural characterization was carried out on the ‘as-received’, casted and heat-treated materials. All composite samples were machined at the bottom edge of the rods (arrows denoted in Figure 1). The cross-section microstructures were investigated using an Optical Microscope (BX60M, Olympus, Japan). Wear

tracks were observed using a Scanning Electron Microscope, SEM (LEO 1450, Leo, UK). Percentage of the reinforced phase was determined using an area fraction method in multiphase function of the AxioVision microscope software (ZEISS, Germany). Results presented were the average values of five different cross-sections.

### Hardness and wear tests

The cross-sections of machined specimens in all conditions were mechanically grinded and polished; hardness was measured using a Rockwell hardness tester (AR-1, Mitutoyo, Japan). The results – expressed in Scale B for ‘as-received’ A356 and in Scale C for composites – were the average of five measurements, presented together with the standard deviation. Wear was tested using a tribometer (Te79, Multi-Axis Tribometer, Phoenix Tribology, UK) following the ball-on-disc method according to ASTM G99 standard testing, with an applied load of 10 N, disk speed of 100 rpm, alumina ball (with hardness of approximately 1,500 HV) size of ¼ in, and pressing time of 1 h. Sliding distance was given at 112.85 m. The mass loss of each sample was measured five times and averaged. Wear rate was calculated by the following equation:

$$W = \frac{M}{\rho D} \quad (3)$$

where  $W$  is wear rate ( $\text{mm}^3/\text{m}$ ),  $M$  is mass loss (g),  $\rho$  is density ( $\text{g}/\text{mm}^3$ ), and  $D$  is sliding distance (m).

Both hardness values and wear rates were subjected to One-way ANOVA analysis using 95% confidence limit.

## RESULTS

### Microstructures of Al-Al<sub>2</sub>O<sub>3</sub> reinforced composites

The microstructure of the ‘as-received’ A356 aluminum alloy is shown in Figure 3. The microstructure consists of  $\alpha$ -Al dendritic and plate-like eutectic Si phases characteristic of casting alloy. Microstructures of the heat-treated composites are shown in Figure 4. All microstructures showed the uniform distribution of alumina particles in aluminum alloy phase. The average area percent of reinforced phase in Al-5wt% Al<sub>2</sub>O<sub>3</sub>, Al-10wt% Al<sub>2</sub>O<sub>3</sub>, and Al-15wt% Al<sub>2</sub>O<sub>3</sub> were approximately  $11.08 \pm 0.37$ ,  $12.58 \pm 0.27$ , and  $15.05 \pm 0.83$  percent, respectively; the phase fraction increased with increasing alumina weight percent.

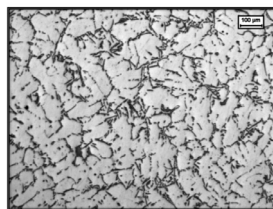


**Figure 3.** ‘As-received’ microstructure of the A356 ingot.

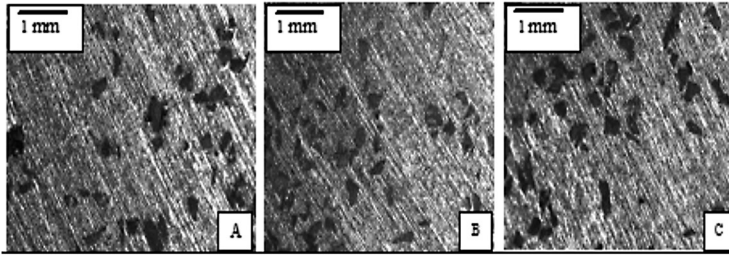


**Figure 4.** Optical micrographs after heat treatment show distribution of alumina particles in the A356 matrix with various alumina weight fractions, together with the average percentage of alumina phase. (A) A356-5wt%  $\text{Al}_2\text{O}_3$  (alumina phase =  $11.08 \pm 0.37\%$ ), (B) A356-10wt%  $\text{Al}_2\text{O}_3$  (alumina phase =  $12.58 \pm 0.27\%$ ), and (C) A356-15wt%  $\text{Al}_2\text{O}_3$  (alumina phase =  $15.05 \pm 0.83\%$ ).

### Hardness testing

The average Rockwell hardness value of A356 aluminum alloy in the ‘as-received’ and heat-treated conditions are shown in Table 3. The average hardness of A356 in ‘as-received’ condition was 23.5 HRB, and increased to 46.0 HRB after heat treatment. Hardness values of composite samples are listed in Table 4; the hardness of the casted composite materials increased with increasing weight percent of alumina phase. The standard deviations of the average hardness values were small, implying that reinforced particles were uniformly distributed in the matrix. From ANOVA test, p-value in the as-casted and T6 conditions were equal to 0.003 and 0.018, respectively, indicating that increasing the percentage of alumina and T6 significantly affected hardness.

**Table 3.** Results of average hardness with standard deviation of A356 in ‘as-received’ and heat-treated conditions.

Specimen	‘As-received’		Heat-treated	
	HRB	SD	HRB	SD
Ingot A356	23.5	1.62	46.0	3.76

**Table 4.** Results of average hardness with standard deviation of composites in casted and heat-treated conditions.

Specimen	Casted		Heat-treated	
	HRC	SD	HRC	SD
A356-5wt% $\text{Al}_2\text{O}_3$	41.3	1.72	46.3	2.14
A356-10wt% $\text{Al}_2\text{O}_3$	44.0	1.26	48.0	1.84
A356-15wt% $\text{Al}_2\text{O}_3$	46.0	1.41	51.1	2.77

### The wear rate after heat treatment of composites

Results of the wear tests are shown in Table 5. The A356-5wt%, 10wt%, and 15wt%  $\text{Al}_2\text{O}_3$  exhibited wear rates of 0.00387, 0.00375, and 0.00350  $\text{mm}^3/\text{m}$ ,

respectively; the differences were not significant. All samples showed very small weight losses and wear rates, indicating all composites had excellent wear resistance. Figure 5A to 5F shows SEM images in SEI mode of no-wear and worn surfaces of the various composites. The micrographs show wear marks clearly as white scratches. The particles were distributed on the surfaces without fracture. The 250  $\mu\text{m}$  alumina particles were uniformly distributed and well bonded with the aluminum matrix.

**Table 5.** Results of the wear tests of the composites after heat treatment.

Specimen	Average mass loss (g/h)	Volume loss ( $\text{mm}^3$ )	Wear rate ( $\text{m}^3/\text{m}$ )
A356-5wt% $\text{Al}_2\text{O}_3$	0.00120	0.43700	0.00387
A356-10wt% $\text{Al}_2\text{O}_3$	0.00118	0.42300	0.00375
A356-15wt% $\text{Al}_2\text{O}_3$	0.00112	0.39500	0.00350

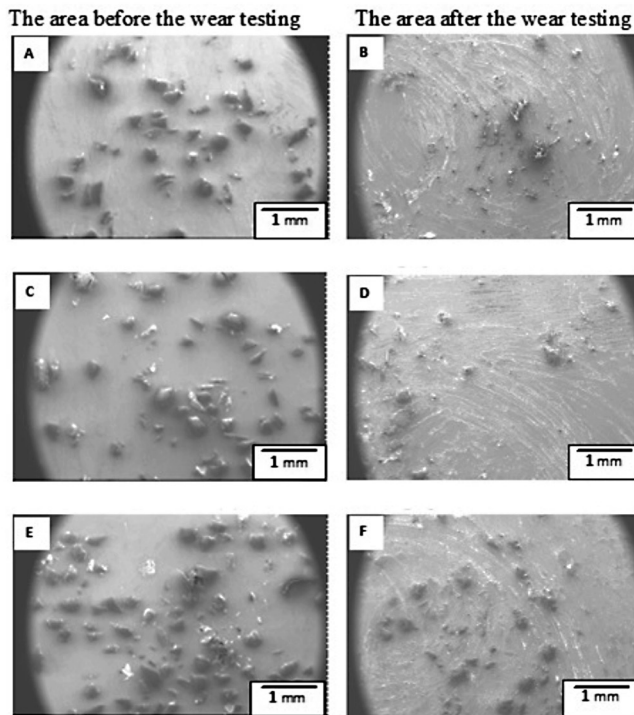


**Figure 5.** SEM images showing surfaces of Al- $\text{Al}_2\text{O}_3$  composites before and after wear tests. (A) A356-5wt%  $\text{Al}_2\text{O}_3$  (before the wear testing), (B) A356-5wt%  $\text{Al}_2\text{O}_3$  (after the wear testing), (C) A356-10wt%  $\text{Al}_2\text{O}_3$  (before the wear testing), (D) A356-10wt%  $\text{Al}_2\text{O}_3$  (after the wear testing), (E) A356-15wt%  $\text{Al}_2\text{O}_3$  (before the wear testing), (F) A356-15wt%  $\text{Al}_2\text{O}_3$  (after the wear testing).

## DISCUSSION

This study fabricated Al-Al<sub>2</sub>O<sub>3</sub> composites using a multi-process regime – sintering, rapid melting, and sand casting. During milling, the chips were mechanically sheared, generating strain within the chips. During sintering at 600°C, the aluminum chips partially welded together. This mechanism allowed the A356 aluminum matrix to better hold the alumina particles together before melting. Another benefit of sintering was the improvement in wettability. To prevent agglomeration and sedimentation of the reinforced phase from the molten matrix, the mix was rapidly melted and poured. The alumina was uniformly distributed in the cross-section area of the composites, as illustrated in Figures 4 and 5. The average reinforced phase fraction analyzed by image analysis of A356-5wt% Al<sub>2</sub>O<sub>3</sub> was higher than the weight percent of alumina particles added, while the hardness values at 10 and 15% were close to the weight percent of alumina particles added, with small uncertainty. This also indicated that the particles were uniformly distributed. As we used simple cylinders only as samples, the effect of shape and size of mold on flowability of the molten composite should be studied further. In addition, chips and sintering technique provide an opportunity to shape composites in solid or semi-solid states.

When casted, the average hardness values of the composites increased with increasing fractions of alumina particles, which indicated that the amount of alumina particles affected hardness. The angular alumina particles obstructed the slip of the slip planes of the matrix, thus increasing the fraction of alumina increased resistance to plastic deformation of the matrix. Alumina particles also promoted dislocation density, due to the thermal expansion coefficient mismatch between the matrix and the reinforced phase. As a result, lattice strains and dislocations developed on cooling.

Hardness of the initial A356 after heat treatment significantly increased, due to formation of an Mg<sub>2</sub>Si precipitated phase, while the hardness values of the composites slightly increased. We attributed the lower aging response of the composites to the reaction between Al<sub>2</sub>O<sub>3</sub> and Mg during melting and casting that resulted in Mg depletion in the matrix. As suggested by Daoud and Reif (2002), Mg in the alloy reacts with imbedded alumina phase via reaction;  $Mg(l) + Al_2O_3(s) \rightarrow MgAl_2O_4(s) + Al(l)$ . MgAl<sub>2</sub>O<sub>4</sub> spinel was found at the interface, resulting in a decreasing amount of magnesium available to form an age hardening phase, such as Mg<sub>2</sub>Si in the matrix. Therefore, hardness of composites with increasing alumina fraction after aging increased slightly; in other words, the smaller amount of alumina fraction more effectively enhanced hardness and resistance to wear. Daoud and Reif (2002) also suggested that to compensate for the MgAl<sub>2</sub>O<sub>4</sub> spinel reaction, more Mg should be added. The effect of MgAl<sub>2</sub>O<sub>4</sub> spinel on matrix/reinforced interface bonding should be studied further. The wear rate of A356-5wt% Al<sub>2</sub>O<sub>3</sub> reduced significantly. Wear resistance of the composites increased with increasing weight fraction of the reinforcing phase. Good wettability of alumina particles led to strong bonds at the interface. Wear rate at higher loads should also be studied further.

## CONCLUSION

In this study, A356 MMCs containing 5, 10, and 15% weight fractions of  $\text{Al}_2\text{O}_3$  particles ( $250\mu\text{m}$ ) as the reinforcement material were produced through sintering, rapid melting, and sand casting. The sintering process improved wettability of alumina and partially bonded the alumina particles before melting. Rapid melting of MMCs without mechanical stirring of the melt prevented aggregation and sedimentation of the reinforcement phase. After casting, alumina particles were uniformly distributed in cross-sections of the composites. The hardness of the casted composites significantly increased as the alumina reinforcement fraction increased. After heat treatment, the hardness of all composite samples increased slightly. The composite materials exhibited a low wear rate, enhancing wear resistance. The wear rate decreased with the increasing fraction of the reinforcement phase.

## ACKNOWLEDGEMENTS

Nattapat Kanchanaruangrong would like to thank the Department of Industrial Management Engineering, Faculty of Industrial Technology, Rajabhat Rajanagarindra University for its scholarship support. The authors would also like to thank the Faculty of Engineering, Ubonratchathani University for its research support and the Department of Industrial Engineering, Faculty of Engineering, Khon Kaen University for the Scanning Electron Microscope session.

## REFERENCES

- Bhansali, K.J, and R. Mehrabian. 1982. Abrasive wear of aluminum-matrix composites. *The Journal of The Minerals, Metals & Materials Society*. September. 34(9): 30-34. doi: 10.1007/BF03338093
- Callister, W. D. 2007. *Materials science and engineering, an introduction*. John Wiley & Sons, New York.
- Donald, R. A., and P. P. Pradeep. 2009. *Essentials of materials science and engineering*. 2<sup>nd</sup> ed.. Thomson Publication. USA.
- Daoud, A., and W. Reif. 2002. Influence of  $\text{Al}_2\text{O}_3$  particulate on the aging response of A356 Al-based composites. *Journal of Materials Processing Technology*. 120(1-3): 313-318. doi: 10.1016/S0924-0136(02)00103-6
- Hashim, J., L. Looney, and M.S.J. Hashmi. 2001. The enhancement of wettability of SiC particles in cast aluminium matrix composites. *Journal of Materials Processing Technology*. 119 (1-3): 329-335. doi: 10.1016/S0924-0136(01)00919-0
- Kok, M. 2005. Production and mechanical properties of  $\text{Al}_2\text{O}_3$  particle-reinforced 2024 aluminium alloy composites. *Journal of Materials Processing Technology*. 161: 381-387. doi: 10.1016/j.jmatprotec.2004.07.068

- Rahimian, M., N. Ehsani, N. Parvin, and H. Baharvandi. 2009. The effect of particle size, sintering temperature and sintering time on the properties of Al-Al<sub>2</sub>O<sub>3</sub> composites, made by powder metallurgy. *Journal of Materials Processing Technology*. 209(14): 5387-5393. doi: 10.1016/j.jmatprotec.2009.04.007
- Stephenson, T.F. 1996. Aluminum hybrid composites containing Nickle-coated graphite particulate, *Processing Properties and Applications of Cast metal Matrix Composites*, eds. P. Rohatgi and P.A.Khan, Warrendale, PA: TMS, 337-351.
- Sujan, D., Z. Oo, M. E. Rahman, M. A. Maleque, and C. K. Tan. 2012. Physio-mechanical properties of aluminium metal matrix composites reinforced with Al<sub>2</sub>O<sub>3</sub> and SiC. *World Academy of Science, Engineering and Technology*. 6: 344-347.
- Telang, A. K., A. Rehman, G. Dixit, and S. Das. 2010. Alternate materials in automobile brake disc applications with emphasis on Al composites – a technical review. *Journal of Engineering Research and Studies*. I(I): 35-46.
- Varuzan M. K., D. Vuk, S. Tomaz, and L. Davorin. 2002. A brake disc in Al-based composite. *Materiali in Technologije*. 36(6): 421-424.
- Zhang, S., and F. Wang. 2007. Comparison of friction and wear performances of brake material dry sliding against two aluminum matrix composites reinforced with different SiC particles. *Journal of Materials Processing Technology*, 182: 122-127. doi: 10.1016/j.jmatprotec.2006.07.018